/pscriptc:/sco4/jobs2/ELSEVIER/gip/week.51/Pgip1387.001101 Mon Jan 14 09:38:36 2002 Page M

ARTICLE IN PRESS

ELSEVIER

Gait and Posture 00 (2001) 000–000

GAIT & POSTURE

www.elsevier.com/locate/gaitpost

Speed dependence of averaged EMG profiles in walking

A.L. Hof [a,b,*], H. Elzinga [b], W. Grimmius [b], J.P.K. Halbertsma [a,b]

[a] *Laboratory of Human Movement Analysis, Department of Rehabilitation, University Hospital Groningen, Groningen, The Netherlands*
[b] *Institute of Human Movement Science, University of Groningen, P.O. Box 196, 9700 Groningen, AD, The Netherlands*

Received 20 April 2001; received in revised form 1 September 2001; accepted 25 November 2001

Abstract

Electromyogram (EMG) profiles strongly depend on walking speed and, in pathological gait, patients do not usually walk at normal speeds. EMG data was collected from 14 muscles in two groups of healthy young subjects who walked at five different speeds ranging from 0.75 to 1.75 ms^{-1}. We found that average EMG profiles varied in a predictable way with speed. The average EMG profile for each muscle at any speed could be estimated in a simple way from two functions, one constant and one proportionally increasing with walking speed. By taking into account the similarity among profiles within functional groups, the number of basic functions could be reduced further. Any average EMG profile among the 14 leg muscles studied at all speeds in the measured range could be predicted from six constant and ten speed-dependent basic patterns. These results can be interpreted in terms of a central pattern generator for human walking. © 2002 Published by Elsevier Science B.V.

Keywords: Electromyogram; Speed dependence; Human walking

1. Introduction

In many gait laboratories surface electromyograms (EMGs) are recorded routinely from patients during gait. A standard procedure is to process the recordings from a number of steps into averaged rectified EMG profiles [1–3]. These averaged profiles can be compared with standard profiles of healthy subjects obtained from the literature, the best known of which is that of Winter [4]. However, Winter's profiles only were collected at one unspecified speed and it is recognised that EMG profiles can change markedly with speed. In view of this, we wished to obtain EMG data recorded at five different speeds to cover the range of walking speeds in healthy subjects.

It is also recognised that the temporal EMG profiles of functionally related muscles can show considerable similarity [5,6]. We also wished to investigate this effect and its relationship to speed dependency to gain insights into the control of muscle activation in automated cyclic movements.

* Corresponding author. Tel.: +31-50-363-2645; fax: +31-50-363-2750.
E-mail address: a.l.hof@med.rug.nl (A.L. Hof).

2. Methods

2.1. Subjects, procedure and normalisation

Averaged EMG profiles were obtained from two groups of nine and 11 healthy young men. The division in two groups had to be made for practical reasons, but care was taken to match the personal data (age 21.9 ± 1.5 years, stature 1.847 ± 0.049 months, leg length 0.984 ± 0.039 months and body mass 75.3 ± 7.8 kg). EMGs of eight muscles were recorded in each group (Table 1). Two muscles, gastrocnemius medialis (GM) and semitendinosus (ST), were recorded in both groups to check whether or not the two groups were comparable.

Subjects walked on a 10 m indoor walkway at speeds of 0.75, 1.00, 1.25, 1.50, and 1.75 ± 0.05 ms^{-1}. Average walking speed was assessed from the interval between passing two infrared beams at both ends of the walkway, 7 m apart. After each round the measured speed was compared with the specified speed and the subjects were instructed to adjust their walking speed accordingly. The walking was repeated until at least ten steps had been recorded at each of the five speeds within ± 0.05 ms^{-1}. Subjects were free to select their stride

0966-6362/02/$ - see front matter © 2002 Published by Elsevier Science B.V.
PII: S0966-6362(01)00206-5

UNCORRECTED PROOF

/pscriptc:/sco4/jobs2/ELSEVIER/gip/week.51/Pgip1387.001101 Mon Jan 14 09:38:36 2002 Page M
ARTICLE IN PRESS

Table 1
List of muscles investigated, with electrode position

		Name	Group	Electrode position	PD
1	SO	Soleus	2	Medial and anterior from Achilles tendon	2/3
2	GM	Gastrocnemius medialis	1,2	Middle of muscle bulge	1/3
3	GL	Gastrocnemius lateralis	1	Middle of muscle bulge	1/3
4	PL	Peroneus longus	2	On line between head of fibula and lateral malleolus	1/4
5	TA	Tibialis anterior	1	Ventral side of lower leg, just lateral from tibia	1/3
6	VM	Vastus medialis	1	Anteromedial muscle bulge thigh	4/5
7	VL	Vastus lateralis	1	Anterolateral muscle bulge thigh	2/3
8	RIF	Rectus femoris	1	Between VM and VL	1/2
9	BF	Biceps femoris, long head	1	Dorsolateral side of thigh	1/2
10	ST	Semitendinosus	1,2	Dorsomedial side of thigh	1/2
11	SM	Semimembranosus	2	In fossa poplitea, between tendons of BF and ST	4/5
12	GX	Gluteus maximus	2	On line between greater trochanter and sacrum	1/2
13	GD	Gluteus medius	2	On line between greater trochanter crista iliaca	1/2
14	AM	Adductor magnus	2	On line between tuberculum pubis and medial epicondylus	1/2

PD, approximate location of the electrodes as a proportion of proximal-distal length.

length. Stride time and time of right toe-off have been given in Table 2.

To avoid the difficulty of including effects due to stature or age, the group of subjects were been chosen as homogeneously as possible. Differences in stature also complicate a comparison of speeds in between subjects. For this reason walking speed v will be expressed in normalised form as $\hat{v} = v/\sqrt{gl_0}$, in which l_0 is leg length and g the acceleration of gravity [7].

2.2. EMG recording

Surface EMGs were recorded bipolarly by Medi-Trace disposable surface electrodes (10×10 mm electrode area, interelectrode distance 24 mm, Graphics Controls, Buffalo NY, USA) with SPA-12 preamplifiers ($100 \times$) directly mounted on the electrodes and a K-Lab postprocessor (K-Lab, Enschede, The Netherlands). The electrode pair was positioned in the lengthwise direction of the muscle. All muscles were recorded from the right leg. Electrode placements were in accordance with recommendations from the literature [8] and from the SENIAM committee [9] and are described in Table 1.

Preamplifier specifications were >110 dB common mode rejection, <2 μV rms noise level and >500 MΩ input impedance. The pre-amplified EMGs were band-pass filtered 20 Hz–10 kHz, third order Butterworth, rectified, and smoothed with a 25 Hz third order Butterworth low-pass filter. Smoothed rectified EMGs were A/D converted at 100 Hz, 12 bits. Rectified EMG values are presented in microvolts as measured at the input. The gain of the complete amplifier and post processing chain was calibrated by an EMG signal generator 'Whisper' (K-Lab). In considering the noise from amplifier and electrodes, and the cross talk from adjacent muscles, it was assumed that smoothed EMG levels below 10 μV could be considered insignificant.

Foot contacts were recorded by aluminium strips taped on heel and toe of the shoes that could make contact with the aluminium walkway.

2.3. Data processing

In a custom made program 'THEWALK' the sampled data were linearly interpolated to 100 points p per stride, triggered by the right heel contact. The recorded steps were screened to exclude those with obvious artefacts or incorrect foot contacts. For every subject i at least ten strides at every speed v were averaged, to give an individual average $e(p, m, \hat{v}, i)$. The $e(p, m, \hat{v}, i)$ of the 9/11 subjects in a group were averaged to obtain a grand mean for each muscle m and normalised speed $\hat{v}$, $E(p, m, \hat{v})$:

$$E(p, m, \hat{v}) = \frac{1}{n_{i=1}^{i=n}} \sum e(p, m, \hat{v}, i) \quad (1)$$

It will be shown in the Section 3, that the 14×5 functions $E(p,m,\hat{v})$ can be approximated by a combination of a much smaller number of functions. The quality of this approximation $E^*(p, m, \hat{v})$ was assessed by determining the rms error between the individual mean

Table 2
Speed, normalised speed, stride time and time of right toe-off

Speed (ms^{-1})	Speed (normalised)	Stride time (s)	RTO (% of stride)
0.75 ± 0.05	0.24 ± 0.02	1.60 ± 0.11	67 ± 1
1.00 ± 0.05	0.32 ± 0.02	1.36 ± 0.06	65 ± 1
1.25 ± 0.05	0.41 ± 0.02	1.18 ± 0.06	64 ± 1
1.50 ± 0.05	0.49 ± 0.02	1.10 ± 0.05	62 ± 1
1.75 ± 0.05	0.57 ± 0.02	1.02 ± 0.04	61 ± 1

UNCORRECTED PROOF

/pscriptc:/sco4/jobs2/ELSEVIER/gip/week.51/Pgip1387.001101 Mon Jan 14 09:38:36 2002 Page M
ARTICLE IN PRESS

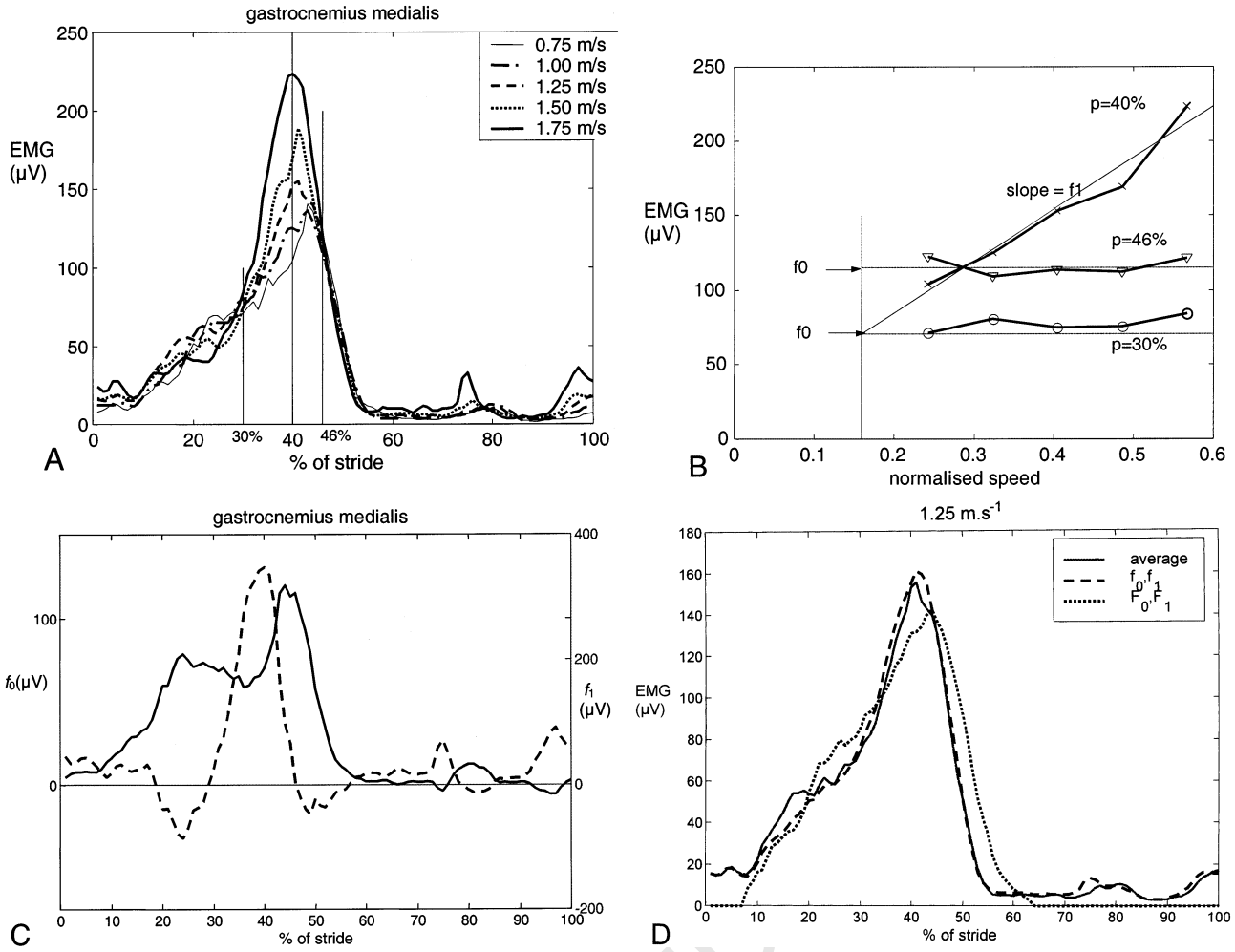

Fig. 1. (a) Averaged EMG profiles for GM muscle in walking at speeds of 0.75, 1.00, 1.25, 1.50, 1.75 ms^{-1} (from bottom to top). (b) Average EMG profile at a single percentage of stride as a function of normalised walking speed. The percentages are: $o-30\%$, $x-40\%$, $\nabla-46\%$. EMG values are either independent of speed, at 30% and 46%, or increase linearly with speed. (c) Functions $f_0(p)$ (thick line) and $f_1(p)$ (dashed) for GM. The function $f_1(p)$ can be interpreted as the slope of the lines in Figure b, for every stride percentage p. The function $f_0(p)$ consists of the intercepts of these lines at the normalised speed 0.16, arrows in Figure b. (d) Quality of the fit of the two estimated profiles. Solid line: average profile of GM at 1.25 ms^{-1}. Dashed line: estimation from $f_0(p)$ and $f_1(p)$, Eq. (4). Dotted line: estimation from F_0 and F_1, Eq. (7). Note that both the F_0 (1) and the F_1 (1) functions used for the GM profile have been derived from the SO profiles.

EMG patterns $e(p, m, i)$, the experimental average $E(p, m, \hat{v})$, and the estimated $E^*(p, m, \hat{v})$, for a single speed $\hat{v}=0.405$, $v=1.25$ ms^{-1}. In order to make the amplitudes of the individual $e(p, m, i)$ comparable, they were normalised. First a gain factor $g(m, i)$ was determined by linear regression without intercept:

$$g(m,i)=\frac{\sum_p (e(p,m,i)E(p,m))}{\sum_p E^2(p,m)} \quad (2)$$

Then the rms error was determined between $e(p, m, i)/g(m, i)$ and $E(p, m)$:

$$\mathrm{rmse}(m,i)=\sqrt{\frac{1}{100}\sum_{p=1}^{100}\left(\frac{e(p,m,i)}{g(m,i)}-E(p,m)\right)^2} \quad (3)$$

and a similar expression for $E^*(p, m)$.

3. Results

The correlation coefficients between the averages for these two groups were between 0.988 and 0.996 for GM and between 0.887 and 0.940 for ST, so that the two groups could be considered comparable.

3.1. EMG-speed relation

The grand average profiles showed considerable changes with speed (Fig. 1a). Parts of the profile increased with speed while other parts did not change. As an example, the relation of three points, for $p=30$, 40 and 46% of stride, in GM muscle, have been plotted as a function of speed in Fig. 1(b). It can be seen that the speed dependency can be well described by linear relations, which could be formulated as:

UNCORRECTED

/pscriptc:/sco4/jobs2/ELSEVIER/gip/week.51/Pgip1387.001101 Mon Jan 14 09:38:36 2002 Page M
ARTICLE IN PRESS

$$E^*(p, m, \hat{v}) = f_0(p, m) + (\hat{v} - 0.16) f_1(p, m) \quad (4)$$

in which $E^*(p, m, \hat{v})$ is the estimated version of $E(p, m, \hat{v})$.

For each muscle, the five $E(p, m, \hat{v})$ functions, at any speed, can thus be predicted by linear interpolation from two functions, f_0 (p, m), the profile at very low speed ($\hat{v} = 0.16$, $v = 0.5$ ms^{-1}) and a function $f_1(p, m)$, denoting the increase of the EMG profile per unit increase of normalised speed, Fig. 1(c and d). The functions were determined by linear regression of the five EMG profiles against speed. The 0.16 factor has been chosen more or less arbitrarily, to give f_0-functions that are always positive. To give an idea of the normalised speeds to be expected, a 'normal' walking speed corresponds to about $\hat{v} = 0.5$. The factor $(\hat{v} - 0.16)$ then amounts to 0.34. For the average leg length of our subjects, 0.98 m, the 'normal' speed equals 1.55 ms^{-1}.

There were two exceptions on the linear increase rule, one for rectus femoris (RF) and one for tibialis anterior (TA) that will be discussed below.

3.2. Correlation between f_0 and f_1 functions

On inspection it was obvious that the f_0 and f_1 *functions* of anatomically related muscles showed considerable resemblance. This could be confirmed by determining the mutual cross correlations. Four groups could be identified, a calf group (soleus (SO), GM, gastrocnemius lateralis (GL) and peroneus longus (PL)), a quadriceps group (vastus medialis (VM), vastus lateralis (VL) and RF), a hamstrings group (biceps femoris (BF), ST and Semimembranosus (SM)) and a gluteal group (gluteus maximus (GX) and gluteus medius (GD)). TA and adductor magnus (AM) did not show high correlations with other muscles.

3.3. Extraction of F_0 and F_1 functions

The high correlations between muscles enabled to condense the 2×14 f_0 and f_1 functions to a smaller set of basic patterns. For most of the non-speed dependent f_0 functions this was fairly straightforward. Each of the calf, quadriceps and hamstrings groups had a characteristic f_0 function. A representative example was selected from within these three groups, from SO, VM and ST, respectively. It was slightly 'edited', by setting parts below the noise limit of 10 μV equal to zero. The same was done with the f_0 functions of GD and AM which could not be grouped. GX had an f_0 function below 10 μV, which was thus set to zero. For the groups, the $f_0(p, m)$ of the remaining muscles in the group were fitted with a constant proportionality factor $D_0(m, k)$ to the example function $F_0(p, k)$ by linear regression with zero intercept:

$$D_0(m, k) = \frac{\sum_p (f_0(p, m) F_0(p, k))}{\sum_p F_0^2(p, k)} \quad (5)$$

Obviously, for the exemplary muscles $D_0(m, k) = 1$. The f_0 function for TA could be composed as a linear combination of the functions F_0 (Eq. (3)), hamstring, F_0 (Eq. (4)), GD stance, and a function of its own, F_0 (Eq. (6)). The resulting matrix D_0 has been given in Table 4. In this way any of the fourteen $f_0(p, m)$ functions could be calculated from the six $F_0(k, p)$ functions by:

$$f_0(p, m) = \sum_k F_0(p, k) D_0(k, m) = \mathbf{F}_0 \mathbf{D}_0' \quad (6)$$

The most appropriate expression is in terms of a matrix multiplication, $\mathbf{D}_0'$ denoting the transpose of $\mathbf{D}_0$. A final filtering with a five-point median filter was performed on the F_0 functions (and on the F_1 and F_2 functions to follow). This filter reduced noise, without affecting the slopes of the profiles. The six F_0 functions have been listed in Table 3 and depicted in Fig. 2(a).

The $F_1(p, k)$ functions, Table 3 and Fig. 2(b), were in principle selected in the same way from the $f_1(p, m)$ functions, but sometimes some intervention was needed. The calf, quadriceps and hamstring group each had a typical burst that occurred in all muscles of the group, $k = 1$, 2 and 3, respectively. Both glutei had a continuous f_1 function, with the highest values in early stance ($k = 4$). The $D_1(m, k)$ factors were determined by the equivalent of (Eq. (5)). TA had a weight acceptance burst typical for that muscle ($k = 6$) and AM an equally typical continuous f_1 function ($k = 7$).

Some bursts could be discriminated that occurred in more than one muscle, but were not exclusively linked to the calf, quadriceps or hamstrings groups. SO and PL showed a prolonged activity in late swing/early stance ($k = 8$). In PL this activity was generally present, in nine out of ten subjects, but in SO it occurred less commonly, in two out of ten cases. SO, PL, TA and GD all showed a swing phase activity ($k = 5$), which has been named 'abductor swing'. SM had an activity in stance not found in the other hamstrings ($k = 7$). GD had, in addition to the common gluteal activity ($k = 8$), an additional weight acceptance peak, similar to those of the quadriceps group ($k = 4$).

BF showed a peak at the onset of swing, around 60%, that did not fit in with the linear relationship (Eq. (1)). It was absent at low, but very prominent at higher speeds. At the intermediate speed of 1.25 ms^{-1} it was present in five out of nine subjects. It was found that this peak could only be fitted in a satisfactory way by a quadratic relationship with speed. This burst was thus placed in a separate F_2 function. The complete fitting function, the combination of (Eqs. (5) and (6)) and then extended with a quadratic term becomes:

UNCORRECTED PROOF

/pscriptc:/sco4/jobs2/ELSEVIER/gip/week.51/Pgip1387.001101 Mon Jan 14 09:38:36 2002 Page M

$$E^*(p, m, \hat{v}) = \mathbf{F}_0\mathbf{D}'_0 + (\hat{v} - 0.16)\mathbf{F}_1\mathbf{D}'_1 + (\hat{v} - 0.16)^2\mathbf{F}_2\mathbf{D}'_2 \quad (7)$$

The $\mathbf{D}_0$, $\mathbf{D}_1$ and $\mathbf{D}_2$ matrices have been given in Table 4.

3.4. Quality of the predicted profiles

Table 5 gives the rms difference between the estimated $E^*(p, m)$ and the measured $E(p, m)$, between the individual profiles $e(p, m, i)$ and $E(p, m)$, average over all subjects, and between $e(p, m, i)$ and $E^*(p, m)$ respectively, all for a single speed of 1.25 ms^{-1}. On inspection, the greater part of the difference between $E^*(p, m)$ and $E(p, m)$ was related to the 'noise level' in the periods of inactivity between the bursts.

Fig. 1(d) gives measured and predicted profiles for GM at 1.25 ms^{-1}. The prediction according to (Eq. (4)) has also been shown.

Fig. 3 shows the averaged EMG profiles for TA muscle in walking at speeds of 0.75, 1.00, 1.25, 1.50, 1.75 ms^{-1} (Table 3a); the same TA profiles, but now filtered with the 3 Hz critically damped low pass filter as described by Winter [4,23] are shown in Table 3(b).

Fig. 4 shows how a neural network that could explain the finding that the EMG profiles can be decomposed into a small number of basic patterns F_0, F_1 and F_2.

4. Discussion

4.1. EMG–speed relation

The approximation (Eq. (4)) was very good, and that by (Eq. (7)) only slightly less (Fig. 1(d) and Table 5). The difference between the measured and the estimated grand mean (first column of Table 5) ranged from 3 to 15 μV rms. It is seen, however, that the differences between the individual EMG profiles and the average profile (second column of Table 5) were in most cases considerably larger, showing that the predicted average profile was only slightly less accurate than the measured average with respect to the individual profiles (third column compared with second). As a consequence, normative EMG profiles for any speed can be obtained by interpolation in this way (Eq. (7)). The availability of normal EMG profiles, closely matched to the actual walking speed, can be helpful in discriminating between normal and abnormal profiles in clinical studies [10]. The only study, to our knowledge, in which EMG profiles have been recorded for a range of speeds is from Nilsson et al. [11] who recorded over a wide range of speeds of 0.4–3 ms^{-1} for walking and 1.0–9 ms^{-1} for running. Many profiles were presented and the global increase of integrated and peak EMG with speed was documented. They did not, however, predict the complete profile from linear regression at every point (Eq. (4)).

The selection of the F_0, F_1 and F_2 patterns from the f_0 and f_1 functions has a subjective component. For the calf, quadriceps and hamstring group we consider the selection reasonably unequivocal. For the majority of muscles of these groups there was only one f_0 and one f_1 function to choose from. Some muscles, SO, RF, SM, had definite additional patterns. For muscles like GD and TA, the profiles of which are included in our proposal of four or five patterns, it is possible that alternative selections might have done equally well.

Table 3
List of F_0, F_1, and F_2 functions, depicted in Fig. 2

	Description	From-to (% of stride)	Peak (μV)	Peak at (%)	From
F_0					
1	Calf stance	8–63	60	46	SO
2	Quad stance	1–47	20	16	VM
3	Hamstrings end swin	91–19	71	0	ST
4	GD stance	0–49	58	12	GD
5	Adductor swin	49–86	22	67–74	AM
6	TA swin	61–100	63	74	TA
F_1					
1	Calf push-off	25–52	295	38–43	SO
2	Quad weight acceptance	79–20	285	4–7	VM
3	Hamstrings late swin	77–98	376	89	ST
4	Glutei	0–100	134	2–8	GX
5	Abductor swin	54–82	113	62	PL
6	TA weight acceptance	80–10	664	0	TA
7	Adductor	0–100	124	10–24, 91	AM
8	SO/PL late swing/early stance	90–19	126	–	SO
9	SM stance	92–51	168	12, 39	SM
F_2	BF early swing	41–70	675	58	BF

UNCORRECTED PROOF

/pscriptc:/sco4/jobs2/ELSEVIER/gip/week.51/Pgip1387.001101 Mon Jan 14 09:38:36 2002 Page M
ARTICLE IN PRESS

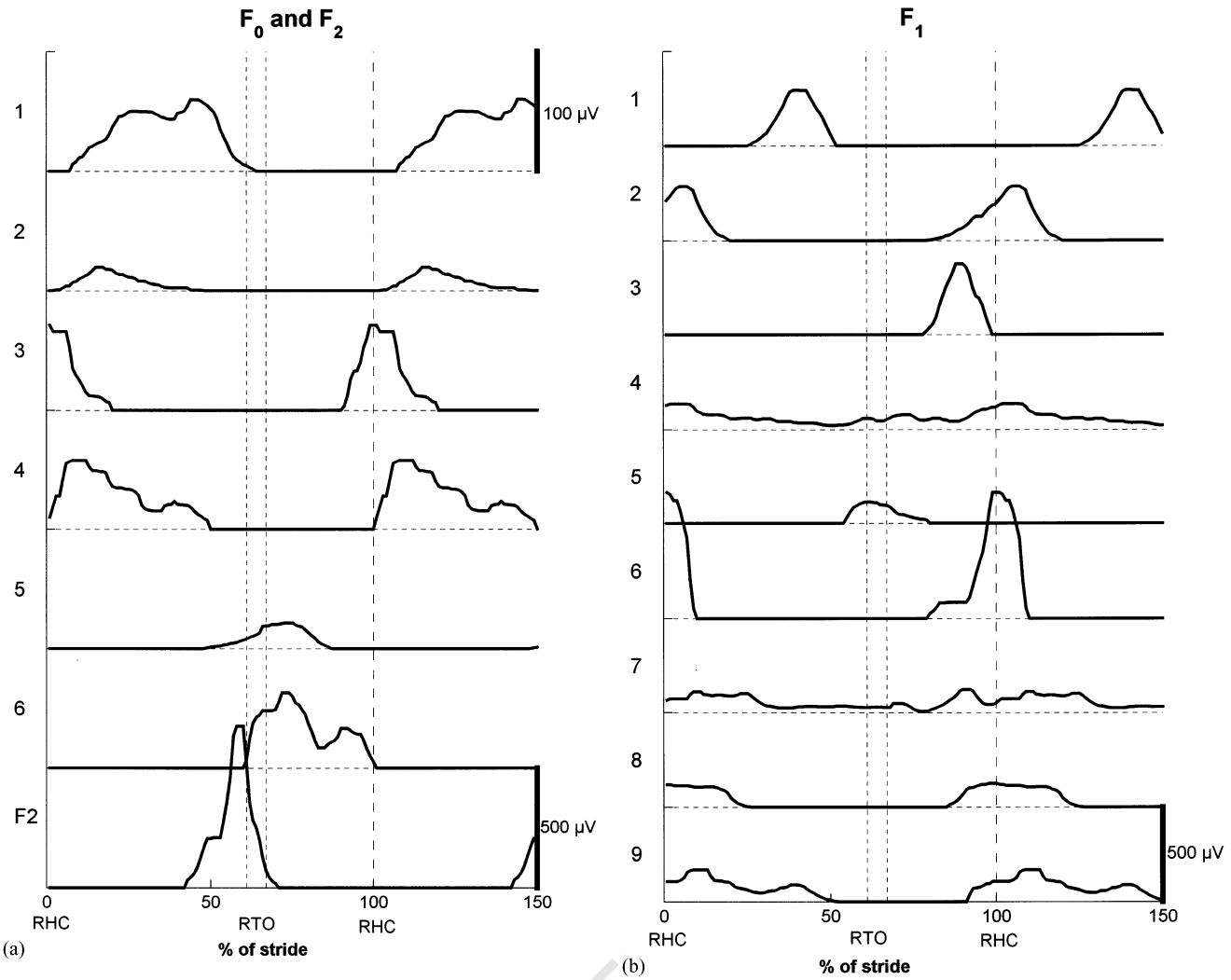

Fig. 2. EMG basic patterns as represented in the F_0, F_1 and F_2 functions. Left: $F_0(p, k)$ and (lowermost) $F_2(p, k)$. Note different scales. Right: F_1 functions. Vertical dashed lines give tome of right heel contact (RHC) = 0 = 100%. Vertical dotted lines give range of right toe-off (RTO). The timing of this event changes with speed (see Table 2). Many of the patterns are high around RHC, for this reason the horizontal scale runs from 0 to 100 to 50%.

The argument of arbitrariness also holds for the proposed nomenclature in Table 3. We have tried to use more or less functional names, where possible to agree with existing nomenclature. Further discussion of the functional interpretation of the various EMG profiles it available in the literature [4,12].

The early swing peak of BF (F_2), with its abnormal quadratic velocity dependence, was recently investigated by Nene et al. [13] who found that it was closely related to shank acceleration. In addition to its function as a hip flexor, RF seems to decelerate the knee flexion in early swing that is initiated by hip flexors and triceps surae that explains why it is apparent at the highest speeds.

A new finding, to our knowledge, is a common 'abductor swing' pattern F_1 (Eq. (5)), which could be discriminated in GD, TA, PL as well as in SO, although at a very low level. Its function might be to give some outward movement of the swing leg. This pattern in SO was not due to cross talk from TA or PL, as the SO electrodes were placed deliberately on the medial side, at a considerable distance from TA and PL. Moreover, in isolated dorsiflexion and eversion, no signal of comparable magnitude was seen. Functionally, SO activity might be an antagonist action against TA and serve to stabilise the ankle in swing.

A further subjective element is the choice of normalised speed 0.16 (0.5 ms^{-1}) as the point at which f_0 is calculated (Eq. (4)). Our main argument is that, with this choice, all f_0 are positive. Another choice is possible, but it would change the form of the f_0 and f_1 functions. A case in point is the glutei. GX has an f_0

/pscriptc:/sco4/jobs2/ELSEVIER/gip/week.51/Pgip1387.001101 Mon Jan 14 09:38:36 2002 Page M
ARTICLE IN PRESS

Table 4
D-matrices

Number		$\mathbf{D}_0$						$\mathbf{D}_1$									$\mathbf{D}_2$
		1	2	3	4	5	6	1	2	3	4	5	6	7	8	9	
1	SO	1	0	0	0	0	0	1			0	0.39	0	0	1		0
2	GM	1.50	0	0	0	0	0	0.83	0	0	0	0	0	1	0	0	0
3	GL	0.25	0	0	0	0	0	0.64	0	0	0	0	0	0	0	0	0
4	PL	0.61	0	0	0	0	0	0.91	0	0	0	1	0	0	1.10	0	0
5	TA	0	0	0.50	0.94	0	1	0	0	0	0	1.72	1	0	0	0	0
6	VM	0	1	0	0	0	0	0	1	0	0	0	0	0	0	0	0
7	VL	0	1.19	0	0	0	0	0	0.84	0	0	0	0	0	0	0	0
8	RF	0	1.31	0	0	0	0	0	0.78	0	0	0	0	0	0	0	0
9	BF	0	0	0.55	0	0	0	0	0	0.44	0	0	0	0	0	0	0
10	ST	0	0	1	0	0	0	0	0	1	0	0	0	0	0	0	0
11	SM	0	0	0.30	0	0	0	0	0	0.58	0	0	0	0	0	1	0
12	GX	0	0	0	0	0	0	0	0	0	0	0	0	0	0	0	0
13	GD	0	0	0	1	0	0	0	0.60	0	1.00	0	0	0	0	0	0
14	AM	0	0 0.22	0	1	1	0	0	0	0	0	1	0	1	0	0	0

See text at Eq. (7). The entries denote: the average EMG profile for, e.g. RF at normalised speed G can be obtained by the addition of 1.31 $F_0(2)+(\hat{v}-0.16)(0.78F_1(2))+(\hat{v}-0.16)^2F_2$.

close to zero, while GD has a distinct pattern F_0 (Eq. (4)). Both have a common F_1 (Eq. (4)) pattern that bears some resemblance to F_0 (Eq. (4)). An alternative description might thus be given, with less basic patterns, but a variable threshold speed. Such a non-linear model would miss the simplicity of the present F_0–F_1 model, however. For extremely low speeds, below 0.5 ms^{-1}, it cannot be expected that the linear speed dependency will hold. An investigation of this speed range may be useful, even if it is questionable whether the EMG patterns at these low speeds can still be called walking patterns (Fig. 3).

4.2. Filtering of rectified EMG

In the earlier study of Winter [4] the EMGs had been filtered by a 3 Hz low-pass filter that simulates muscle mechanical properties, with the effect that the filtered EMG looks similar to the isometric muscle force [14,15]. This is very instructive, but has a number of drawbacks. First, the temporal characteristics of the EMG profiles are rather 'smeared out'. From our results it is seen that several profiles show very abrupt endings, such as GM at 50% (Fig. 1) or TA at 7% (Fig. 3a). The TA decline amounted to a 50% decrease over 1% of the cycle. This is half the falling rate of the smoothing filter (3rd order Butterworth, 25 Hz) applied here. In addition, a timing error of the foot contact due to the 100 Hz sampling frequency of ± 5 ms should be taken into account. The conclusion is that the cut-off frequency of low-pass filter cannot be made much lower than 25 Hz without degrading the fastest transients of the rectified EMG in human leg muscles. A second argument against 3 Hz filtering is that muscle actions in walking are in general not isometric in the sense that origin-insertion length changes and speeds are small with respect to the force–length and force–velocity relations of the muscles [15]. When preferred, the 3 Hz filtering can still be applied to the $E^*(p, m)$ signal afterwards cf. Fig. 3(b). When this is done, a comparison with the data of Winter [4] is possible. The general form and timing of all profiles showed good agreement, but the amplitude of Winter's profiles was 1.3 to 3.5 times higher (Fig. 4)

Table 5
Root-mean-square errors, from left to right

Muscle		$E-E^*$ (μV_{rms})	$e-E^*$ (μV_{rms})	$e-E^*$ (μV_{rms})
1	SO	7.0	15.2	16.4
2	GM	14.7	16.5	21.1
3	GL	7.2	5.0	8.6
4	PL	10.6	17.1	18.7
5	TA	14.4	29.0	32.0
6	VM	3.3	7.0	7.7
7	VL	5.2	8.7	9.7
8	RIF	11.7	14.4	18.5
9	BF	8.4	9.2	12.1
10	ST	8.6	13.3	15.8
11	SM	11.8	9.5	14.6
12	GX	4.2	6.5	7.6
13	GD	13.5	16.9	21.5
14	AM	6.3	8.9	10.3

(a) Between average EMG profile $E(p, m)$ calculated from the data and the profile predicted from F_0, F_1 and F_2, $E^*(p, m)$; (b) between the individual EMG profiles $e(p, m, i)$ and $E(p, m)$, mean for all subjects; and (c) between the individual EMG profiles $e(p, m, i)$ and $E^*(p, m)$, mean for all subjects. Data have been calculated for a speed of 1.25 ms^{-1} (normalised speed 0.40). Errors as a rule increased with speed, in line with the increase of the EMG levels.

UNCORRECTED PROOF

/pscriptc:/sco4/jobs2/ELSEVIER/gip/week.51/Pgip1387.001101 Mon Jan 14 09:38:36 2002 Page M

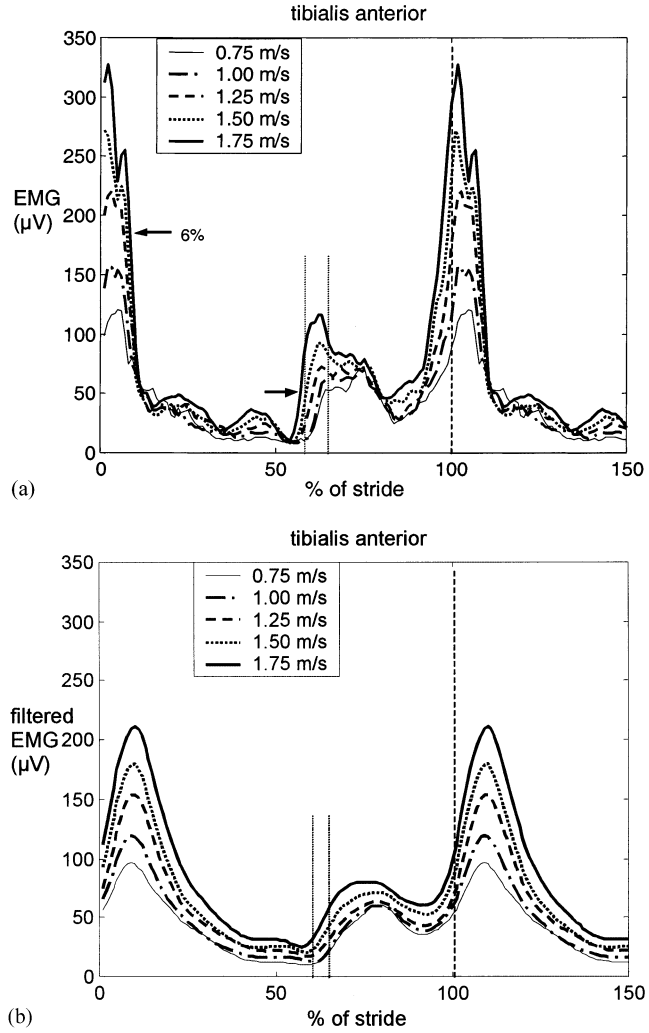

Fig. 3. Averaged EMG profiles for TA muscle in walking at speeds of 0.75, 1.00, 1.25, 1.50, 1.75 ms^{-1} (from bottom to top). Note the steep edge around 6%, which is very reproducible across speeds. The onset of activity just before swing advances from 63 to 56% with speed. This is the only example found in our data of a shift in timing that could not be explained by the increase of the F_1 pattern with speed. EMGs were filtered after rectifying by a 25 Hz third order Butterworth low-pass filter. Vertical dashed lines give time of right heel contact (RHC) = 0 = 100%. Vertical dotted lines give range of right toe-off (RTO). The timing of his event changes with speed (see Table 2). (b) Same TA profiles, but now filtered with the 3 Hz critically damped low pass filter as described by Winter [4,23].

4.3. Central pattern generator

The finding that the EMG profiles of many muscles at a wide range of speeds can be represented by addition of few basic patterns is consistent with the notion of a central pattern generator (CPG) for human walking. Convincing evidence for such a CPG in vertebrates is well established [16,17], but its importance for human gait is still debated [18]. The EMG findings in this paper are too indirect to give more than supporting evidence on the existence of some form of CPG in humans. On the other hand, when such a CPG is assumed, it explains some phenomena that are much harder to interpret with alternative schemes of motor control.

Fig. 4 shows the diagram of a neural configuration that is able to represent the experimental findings as summarised in (Eq. (7)). Two higher commands descend to the CPG, one on/off command 'walk', and one graded 'speed' command. These two commands each drive a number of cell groups bursting at fixed phases of the gait cycle, representing the six F_0 and ten F_1 and F_2 functions, respectively. These cell groups are mutually connected to ensure that the cycle is completed in a fixed order and at fixed relative timing within the cycle. The cycle, in its turn, is time-locked by sensory input to the mechanical movement. Finally, sensory feedback ensures that adequate reflexes counteract disturbances. It has been shown in theoretical studies that a neural network with these properties can indeed generate stable two-legged locomotion [19].

One aspect of such a CPG scheme is not apparent from the presented EMG data: the role of reflexes. It is well established [18,20,21] that the activity of many leg muscles in locomotion is in part due to reflexes, the gains of which are modulated in the course of the gait cycle. The EMG profiles represent averages over many steps and many subjects. Average EMG profiles can only give the average activity, and cannot discriminate whether the activity was directly programmed or resulted from indirect reflex action.

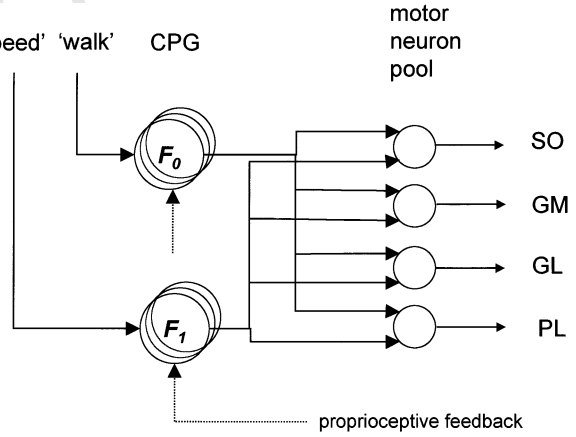

Fig. 4. Neural network that can explain the finding that the EMG profiles can be decomposed into a small number of basic patterns F_0, F_1 and F_2. A Central Pattern Generator is assumed that consists of two sets of half-centres bursting at specific intervals of the walking cycle. One set, corresponds to the F_0 patterns and is activated by a on/off signal 'walk'. The other set corresponds to the F_1 and F_2 patterns and is activated by a graded signal 'speed'. The outputs of both half-centres connect to the ipsilateral motor unit pool, with synaptic loadings proportional to the entries in the $\mathbf{D}_0$, $\mathbf{D}_1$ and $\mathbf{D}_2$ matrices. It is supposed that there is proprioceptive feedback to correct for disturbances and to time-lock the CPG cycle to the actual movement. An identical set of half-centres, running in counterphase, is assumed for the contralateral side.

UNCORRECTED PROOF

/pscriptc:/sco4/jobs2/ELSEVIER/gip/week.51/Pgip1387.001101 Mon Jan 14 09:38:36 2002 Page M

An effect that can be explained by a CPG model is the finding that the relative timing of the EMG profiles did not change with speed. At higher stride frequency the patterns are just played faster, but they did not shift in phase. This in spite of stride time decreasing from 1.6 to 1.0 s from the lowest to the highest speed (Table 2). The advancement, for example, of GM activity with speed (Fig. 1a) can be completely explained by the increase of the F_1 (Eq. (1)) pattern with speed. In the muscles investigated only one exception to the rule of constant relative timing has been found, the TA activity in swing, see Fig. 4(a). The onset of this pattern F_0 (Eq. (6)) advanced from 63 to 56% with a speed increase from 0.75 to 1.75 ms^{-1}, in all cases 4–5% before right toe-off (cf. Table 2).

A second finding in agreement with a CPG is the fact that related muscle groups showed activity profiles that were composed of the same basic patterns, but in a different proportion. For example, the profiles of the calf group, SO, GM, GL, PL all contained the patterns F_0 (1) and F_1 (1), but the respective entries in $\mathbf{D}_0$ and $\mathbf{D}_1$ were different. Similar effects were seen for the vasti and hamstring groups.

Varraine et al. [22] instructed subjects to make one extra long or extra short step when walking on a treadmill. Our CPG model (Fig. 4) would predict the modulations in the EMG profiles they report are very similar to what would be expected from a temporary modulation of the F_1 patterns.

The main purpose of this paper was to present a set of normal EMG profiles, covering the usual range of walking speeds for use in clinical studies. Nevertheless, it is hoped that the decomposition into a small set of basic patterns, as presented here, may serve further in understanding motor control in human walking.

References

[1] Shiavi R, Green N. Ensemble averaging of locomotor electromyographic patterns using interpolation. Med Biol Eng Comput 1983;21:573–8.
[2] Yang J, Winter D. Surface EMG profiles during different walking cadences in humans. Electroenceph Clin Neurophysiol 1985;60:485–91.
[3] Kleissen R, Hermens H, den Exter T, de Kreek J, Zilvold G. Simultaneous measurement of surface EMG and movements for clinical use. Med Biol Eng Comput 1989;27:291–7.
[4] Winter DA. The biomechanics and motor control of human gait, second ed. Waterloo, Canada: University of Waterloo Press, 1991.
[5] Davis B, Vaughan C. Phasic behavior of EMG signals during gait: use of multivariate statistics. J Electromyogra Kinesiol 1993;3:51–60.
[6] Olree K, Vaughan C. Fundamental patterns of bilateral muscle activity in human locomotion. Biol Cybern 1995;73:409–14.
[7] Hof AL. Scaling gait data to body size. Gait Posture 1996;4:222–3.
[8] Perotto A. Anatomical guide for the electromyographer. The limbs and the trunk. Springfield: CC Thomas, 1994.
[9] Freriks B, Hermens H, Disselhorst-Klug C, Rau G. The recommendations for sensors and sensor placement procedures for surface electromyography. In: Hermens H, editor. European recommendations for surface electromyography. Enschede: Roessingh Research and Development, 1999:15–53.
[10] Boerboom AL, Hof AL, Halbertsma JPK, van Raaij JJAM, Schenk W, Diercks R, van Horn JR. Atypical hamstrings electromyographic activity as a compensatory mechanism in anterior cruciate ligament deficiency. Knee Surg Sports Traumatol Arthrosc 2001;9:211–6.
[11] Nilsson J, Thorstensson A, Halbertsma J. Changes in leg movements and muscle activity with speed of locomotion and mode of progression in humans. Acta Physiol Scand 1985;123:457–75.
[12] Inman VT, Ralston HJ, Todd F. Human walking. Baltimore: Williams and Wilkins, 1981.
[13] Nene A, Mayagoitia R, Veltink P. Assessment of rectus femoris function during initial swing phase. Gait Posture 1999;9:1–9.
[14] Coggshall JC, Bekey GA. The relationship between the surface EMG and force transients in muscle: simulation and experimental studies. Med Biol Eng Comput 1970;8:265–70.
[15] Hof AL. The relationship between electromyogram and muscle force. Sportverletz-Sportschad 1997;11:79–86.
[16] Grillner S. Control of locomotion in bipeds, tetrapods, and fish. In: Brooks V, editor. Handbook of physiology, the nervous system II. Motor control. Bethesda: American Physiological Society, 1981:1179–236.
[17] Kjaerulff O, Kiehn O. Distribution of networks generating and coordinating locomotor activity in the neonatal rat spinal cord in vitro: a lesion study. J Neurosci 1996;16:5777–94.
[18] Duysens J, van de Crommert H. Neural control of locomotion; Part 1: the central pattern generator from cats to humans. Gait Posture 1998;7:131–41.
[19] Taga GA. A model of the neuro–musculo–skeletal system for human locomotion emergence of basic gait. Biol Cybern 1995;73:97–111.
[20] Capaday C, Stein RB. Amplitude modulation of the soleus H-reflex in the human during walking and standing. J Neurosci 1986;6:1308–13.
[21] Duysens J, Clarac F, Cruse H. Load-regulating mechanisms in gait and posture: comparative aspects. Physiol Revs 2000;80:83–133.
[22] Varraine E, Bonnard M, Pailhous J. Intentional on-line adaptation of stride length in human walking. Exp Brain Res 2000;130:248–57.
[23] Winter A, Patla A. Signal processing and linear systems for the movement sciences. Waterloo: Waterloo Biomechanics, 1997.

UNCORRECTED PROOF